HHS Public Access

Author manuscript

Sci Signal. Author manuscript; available in PMC 2023 December 21.

Published in final edited form as:

Sci Signal. 2023 November 21; 16(812): eadg1668. doi:10.1126/scisignal.adg1668.

Enteric glia promote visceral hypersensitivity during inflammation through intercellular signaling with gut nociceptors

Wilmarie Morales-Soto[1], **Jacques Gonzales**[1], **William F. Jackson**[2], **Brian D. Gulbransen**[1,*]

[1]Department of Physiology, Neuroscience Program, Michigan State University, East Lansing, MI, 48824 USA.

[2]Department of Pharmacology and Toxicology, Michigan State University, East Lansing, MI, 48824 USA.

Abstract

Inflammation in the intestines causes abdominal pain that is challenging to manage. The terminals of sensory neurons innervating the gut are surrounded by glia. Here, using a mouse model of acute colitis, we found that enteric glia contribute to visceral pain by secreting factors that sensitized sensory nerves innervating the gut in response to inflammation. Acute colitis induced a transient increase in the production of proinflammatory cytokines in the intestines of male and female mice. Of these, IL-1β was produced in part by glia and augmented the opening of the intercellular communication hemichannel connexin-43 in glia, which made normally innocuous stimuli painful in female mice. Chemogenetic glial activation paired with calcium imaging in nerve terminals demonstrated that glia sensitized gut-innervating nociceptors only under inflammatory conditions. This inflammatory, glial-driven visceral hypersensitivity involved an increased abundance of the enzyme COX-2 in glia, resulting in greater production and release of prostaglandin E2 which activated EP_4 receptors on sensory nerve terminals. Blocking EP_4 receptors reduced nociceptor sensitivity in response to glial stimulation in tissue samples from colitis-model mice, and impairing glial connexin-43 reduced visceral hypersensitivity induced by IL-1β in female mice. The findings suggest that therapies targeting enteric glial-neuron signaling might alleviate visceral pain caused by inflammatory disorders.

INTRODUCTION

Abdominal pain is a common gastrointestinal symptom and a feature of various intestinal disorders, including irritable bowel syndrome (IBS) and inflammatory bowel disease (IBD) (1, 2). Treating pain remains difficult due to the poor understanding of the underlying mechanisms. The most prevalent theory describing the etiology of abdominal pain is that acute inflammation promotes visceral hypersensitivity (3), which contributes to abdominal

*Corresponding author. gulbrans@msu.edu.

Author Contributions: Study concept and design: BDG and WMS; acquisition of data: WMS, JG, and WFJ; analysis and interpretation of data: WMS, JG, WFJ, and BDG; drafting of the manuscript: WMS; critical revision of the manuscript: WMS, JG, WFJ, and BDG; statistical analysis: WMS; acquisition of funding: BDG and WMS.

Competing Interests: The authors declare that they have no competing interests.

pain by facilitating nociceptive signaling along the gut-brain axis (4). This mechanism is considered relevant to pain in IBS and IBD in remission because despite being different clinical entities, there is substantial overlap between these conditions, and both are associated with bouts of inflammation (5, 6). Visceral hypersensitivity can be caused by changes at multiple points along the ascending and descending neural pathways that transduce nociceptive information from the periphery; however, changes in the sensitivity of nerve fibers that innervate the intestine is considered a primary cause and an attractive therapeutic target (7).

Nociceptive information in the gut is transduced by the peripheral axon terminals of primary afferent neurons that express the transient receptor potential cation channel subfamily V member 1 (TRPV1) and are sensitized during acute inflammation (8, 9). Nociceptor sensitization can lead to enhanced sensations of painful stimuli (hyperalgesia) and/or painful sensations in response to normally innocuous stimuli (allodynia). Mechanisms responsible for these phenomena are thought to involve mediators released by immune cells such as mast cells that act on afferent nerve terminals (10). However, this theory has been questioned because mast cell numbers are inconsistent in IBS (11) and is at odds with the anatomical arrangement of nerve fibers and mast cells in the gut wall (12). Mast cells are predominantly associated with mucosal afferents, which comprise only 10% of afferent terminals in the colon (13–15). Sensitization of mucosal afferents could contribute to hyperalgesia but would not explain allodynia, which involves the sensitization of high threshold nerves that densely innervate the myenteric plexus and muscularis where mast cells are rare (15). Therefore, additional mechanisms must be active at the level of the myenteric plexus that contribute visceral hypersensitivity.

Nociceptors innervating the myenteric plexus are surrounded by enteric glia (2, 16). Communication between enteric glia, neurons, and immune cells has emerged as an important mechanism that modulates neural-controlled gut functions (17, 18) as well as neuroimmune interactions and neuroinflammatory responses (19, 20). Enteric neuroinflammation is driven by processes that involve nociceptor-to-enteric glia signaling (2), but whether glia have reciprocal effects on nociceptive nerve sensitivity is unclear. Related populations of glia in the central nervous system have well defined roles in promoting synaptic plasticity (21) and sensitization of central pain pathways (22). Interactome gene analysis data suggest that enteric glia could have similar roles in the gut because glial genes upregulated during inflammation are linked to downstream pain-promoting mechanisms in colon-projecting nociceptors (23). While enteric glia are known to contribute to chronic visceral hypersensitivity through interactions with immune cells (20), how they might directly influence nociceptive nerve terminal sensitivity remains unknown.

The goal of this study was to test the hypothesis that enteric glia contribute to visceral hypersensitivity by regulating the sensitivity of nociceptive nerve terminals innervating the intestine. To this end, we developed tools to measure visceral nociceptor activity in real time in the intestine and used glial-specific perturbations to test the impact of glial signaling on nociceptor sensitivity in the contexts of health and inflammation. Our results uncover a unique mechanism whereby enteric glia sensitize visceral afferent nerve terminals in the myenteric plexus. The molecular mechanisms underlying glial-mediated nociceptor

sensitization identified here address a critical gap in understanding mechanisms that lead to visceral pain and highlight enteric glia as a potential target for cell-specific therapies.

RESULTS

Enteric glia contribute to the inflammatory milieu that drives visceral hypersensitivity

Acute inflammation produces visceral hypersensitivity in mice and humans (3) by disrupting the balance between pro- and anti-inflammatory mediators (24) that can sensitize and/or activate visceral nociceptors (3, 20). The sensitizing effects of proinflammatory mediators on nociceptors is often studied in the preclinical mouse model of DNBS-induced colitis due to its translational relevance and reproducibility (25). Thus, first, we characterized the inflammatory profile in this model. Male and female mice treated with DNBS were monitored for disease progression by tracking changes in weight and macroscopic tissue damage (26). Weight loss progressed during the first 72 hours following DNBS treatment, and recovered to control levels by 3 weeks (fig. S1, A and C). Similarly, macroscopic damage was evident at 6 hours after DNBS treatment, peaked by 48 hours and resolved by 3 weeks (Fig. S1, B and D). To determine which pro-inflammatory mediators are present during nociceptor sensitization, we performed a comprehensive multiplex immune assay on whole colon samples from male and female mice across the time course of DNBS-induced colitis (Fig. 1A and data file S1). The abundance of several pro-inflammatory cytokines were increased in the colon at 6 and 48 hours after colitis induction (at early and peak inflammation, respectively), of which most returned to baseline levels over the following 3 weeks (the resolution phase of this colitis model). Notably, levels of key cytokines implicated in the pathogenesis of GI disorders (27) and pain hypersensitivity (21) were increased in both males and females at 6 and 48 hours after DNBS treatment (Fig. 1B). Increases in interleukin 1-β (IL-1β) and IL-6 were prominent at 6 hours after treatment, both showing levels over 100 times higher than controls in males and females. The levels of tumor necrosis factor-α (TNF-α) increased over 70-fold at 48 hours in females and 17-fold in males, although it did not reach statistical significance in the latter. Similarly, interleukin-17 (IL-17) was increased in the colon of males at 6 hours and females at 48 hours. The abundance of interferon-γ (IFN-γ) in the colon decreased in males at 6 hours, and no change was observed in females. Analysis of published bulk RNA-sequencing data of enteric glia from mice at peak colitis (2) showed that pathways associated with these cytokines were significantly upregulated in enteric glia (Fig. 1C). Notably, production of IL-1β and IL-6 as well as associated receptors were upregulated in enteric glia in response to DNBS exposure. IL-1β production contributes to visceral hypersensitivity by directly modulating nociceptive nerves (3, 21), and our data (Fig. 1A-C) suggest that enteric glia are a potential source of IL-1β surrounding nociceptors. In support, immunolabeling showed a 45% increase in IL-1β protein expression in myenteric glia during DNBS-induced colitis (Fig. 1, D and E).

Proinflammatory cytokines facilitate glial Cx43 hemichannel gating

In the CNS, proinflammatory cytokines contribute to chronic pain through effects on glial connexin-43 (Cx43) hemichannels (22). Enteric glia express Cx43 hemichannels, and Cx43-mediated signaling regulates intercellular communication (18, 28) and associated GI

functions (26). To explore how proinflammatory mediators affect enteric glial Cx43 activity, we assessed cellular uptake of the intercalating agent ethidium bromide (EtBr), a selective method to measure Cx43 hemichannel opening in glia (29) in distal colon tissue preparations from male and female mice. We initially tested the singular effects of proinflammatory cytokines on Cx43-mediated dye uptake. Glial Cx43 hemichannel opening was increased in the presence of proinflammatory cytokines in the myenteric plexus of both male (Fig. 2, A and B) and female (Fig. 2, C and D) mice. Incubation with IL-17 had no impact on dye uptake, whereas IL-1β, IL-6, IFN-γ, and TNF-α induced a robust increase in glial EtBr fluorescence when compared to controls. Therefore, cytokines that were upregulated during active inflammation increased Cx43 hemichannel activity in otherwise unstimulated enteric glia. Comparing the data from males and females did not indicate significant sex differences in the effects of cytokines on glial Cx43 hemichannels (table S2); therefore, data from subsequent experiments included pooled data from both sexes.

Cx43-dependent EtBr uptake in enteric glia increases following purinergic stimulation with the $P2Y_1$ agonist ADP (Fig. 3A), which contributes to colitis (26, 28). Thus, we investigated how proinflammatory cytokines affect Cx43 opening in enteric glia following purinergic activation. Treatment with ADP increased EtBr uptake by approximately 30% (Fig. 3B, and fig. S2), confirming that this paradigm was efficient at activating enteric glia and stimulating Cx43 hemichannel opening. Application of IL-17, IFN-γ, or TNF-α had no effect on EtBr dye uptake in ADP-stimulated glia (fig. S2, B to D). In contrast, IL-1β (Fig. 3, A and B) and IL-6 (fig. S2A) potentiated dye uptake in ADP-stimulated glia by approximately 24 and 50%, respectively. These effects of IL-1β and IL-6 were dependent on Cx43, as their actions were diminished by blocking Cx43 hemichannels with the mimetic peptide 43Gap26 (Fig. 3, A and B, and fig. S2A). IL-1β-mediated potentiation of dye uptake was absent in the presence of the pore-channel blocker Gd (Fig. 3B), which ruled out potential channel-independent effects. Likewise, repeating the ADP and IL-1β experiments in tissue preparations from mice with targeted deletion of glial Cx43 ($Sox10^{CreERT2};Cx43^{f/f}$) (30) showed that IL-1β was unable to potentiate EtBr dye uptake in either quiescent or stimulated glia in the absence of Cx43 (Fig. 3C). Dye uptake was independent of pannexin-1 channels in enteric neurons (31) and was unaffected by the mimetic peptide 10Panx (Fig. 3B). Thus, IL-1β may facilitate mechanisms involved in the release of neuroactive substances from glia.

Enteric glia sensitize nociceptors through Cx43-dependent mechanisms in proinflammatory conditions

Enteric glial Cx43 signaling is active during the acute phase of colitis when the sensitization of nociceptors occurs (2, 22, 32). Enteric glia display a tight anatomical and functional relationship with $TRPV1^+$ nociceptors (2), as demonstrated by co-labeling enteric glia and TRPV1-positive nerve fibers within myenteric ganglia in the mouse colon (Fig. 4A), suggesting that glial activation could affect nociceptor activity. To test how glial signaling influences nociceptor sensitivity, we conducted Ca^{2+} imaging in $Trpv1^{Cre;GCaMP5g\text{-}tdT}$ mice. This line conditionally expresses the genetically encoded Ca^{2+} indicator GCaMP5g in $TRPV1^+$ nerves (Fig. 4B), enabling the assessment of the activity of nociceptive nerve terminals in the gut wall itself (Fig. 4B). Whereas most GCaMP and tdTomato expression are confined to extrinsic nerves in this mouse line, some myenteric neurons also display

reporter expression (fig. S3A). However, enteric neurons expressing tdTomato and GCaMP were unresponsive to capsaicin (fig. S3B), supporting previous data showing that enteric neurons do not express functional TRPV1 in adult animals (33). Therefore, nerve-fiber Ca^{2+} responses observed in this line primarily reflect responses in extrinsic nociceptors that innervate the myenteric plexus.

Nociceptor sensitivity was assessed by measuring Ca^{2+} responses evoked by the TRPV1 agonist capsaicin (Fig. 4C). Effects of glial activation were studied by stimulating glia with the $P2Y_1$ agonist ADP and by blocking downstream glial Cx43 hemichannel-mediated transmitter release with the mimetic peptide 43Gap26 (Fig. 4B). $TRPV1^+$ nerve fibers exhibited robust responses to capsaicin in control preparations, and stimulating glia with ADP did not activate nerve fibers or alter their responses to capsaicin under basal conditions (Fig. 4D). However, ADP increased nociceptor responses to capsaicin in the presence of IL-1β by ~60% (Fig. 4E, F). This effect required glial activation by ADP, because treatment with IL-1β alone had no effect on capsaicin responses in nociceptors (Fig. 4F). Nociceptor sensitization by ADP also required glial Cx43 and was blocked in the presence of 43Gap26 (Fig. 4F). Therefore, purinergic activation of glia sensitizes nociceptive nerves in the intestine through Cx43-dependent signaling during inflammation.

PGE_2 is a glial-derived mediator that sensitizes $TRPV1^+$ nociceptors

Our Ca^{2+} imaging studies in *Trpv1*$^{Cre;GCaMP5g\text{-}tdT}$ mice showed that enteric glia sensitize $TRPV1^+$ nociceptors through Cx43-dependent mechanisms. Cx43 controls glial intercellular communication by regulating the production of mediators such as prostaglandin E2 (PGE_2) (34). PGE_2 production is increased during inflammation and facilitates nociceptive transmission through actions on EP_4 receptors expressed by visceral nociceptors (35). Thus, we speculated that glial PGE_2 release mediates the sensitizing effects of glial activation on $TRPV1^+$ nociceptors.

Analysis of glial RNA-sequencing data (2) showed that enteric glia express several genes associated with PGE_2 synthesis and regulation. Notably, there is a 6-fold increase in the expression of the gene encoding cyclooxygenase-2 (COX-2; *Ptgs2*) in enteric glia during peak colitis in mice (Fig. 5A). To confirm these data, we performed *in situ* hybridization for *Ptgs2* transcripts in colon whole mounts from control and inflamed (DNBS-treated) mice. *Ptgs2* RNA abundance was increased relative to control samples at 48 hours after DNBS treatment (Fig. 5B). Increased *Ptgs2* expression colocalized with Sox10-positive glia but not with peripherin-positive neurons within myenteric ganglia, indicating that enteric glia are the main cellular site of PGE_2 production in myenteric ganglia during acute inflammation. To provide direct evidence of glial PGE_2 release, we quantified PGE_2 release from primary cultures of enteric glia derived from the mouse colon (Fig. 6A). Stimulating enteric glial cultures with ADP increased PGE_2 release in the presence of IL-1β (Fig. 6B). This effect required glial Cx43 hemichannel opening, because it was blocked by 43Gap26 (Fig. 6B). These data show that COX-2 activity in enteric glia and their subsequent PGE_2 production has the potential to promote enteric neuroplasticity during inflammation (36).

PGE_2 is a ubiquitous molecule that is released by multiple cell types including mast cells, which also modulate visceral hypersensitivity (10). Mast cells are mainly present at the

level of the mucosa and are rare at the levels of the myenteric plexus and muscularis where high threshold afferent terminals are located (13, 15). To determine relative potential contributions of mast cells and glia, we quantified mast cells at the level of the myenteric plexus in mast cell reporter (*MCPT5*$^{Cre;GCaMP5g\text{-}tdT}$) mice (37) and assessed glial numbers by Sox10 immunolabeling within myenteric ganglia of WT mice. Average mast cell density in the distal colon myenteric plexus was significantly lower than the density of Sox10+ glia in the same region (Fig. 7, A to C). These counts show that glia outnumber mast cells in regions surrounding afferent terminals by a factor of at least 2:1. Similarly, other immune cells such as neutrophils can contribute to the available pool of PGE_2 during inflammation (38). To assess the distribution of neutrophils in the colon during colitis, we performed immunohistochemistry with Lymphocyte antigen 6 complex locus G6D (Ly6G) in cross sections of mice treated with saline or DNBS for 48 hours (fig. S4). In healthy controls, Ly6G+ cells were mainly confined to the mucosa. The abundance of Ly6G+ cells increased following DNBS colitis, but most Ly6G+ cells remained located within the mucosa. Minimal neutrophil labeling was observed within the myenteric plexus where glial labeling with GFAP was most abundant. Therefore, glia appear to be the predominant PGE_2-producing cells surrounding nociceptive nerve terminals in the myenteric plexus.

Our Ca^{2+} imaging data above (Fig. 4) show that purinergic activation of enteric glia modulates nociceptive signaling through Cx43-dependent mechanisms. However, it is possible that $P2Y_1$ receptor expression by afferent (39) and enteric neurons (40) or immune cells (41) could complicate our interpretations. To circumvent this issue, we developed a dual chemogenetic and optogenetic reporter mouse model, *Trpv1*$^{Cre;GCaMP5gtdT}$*;GFAP-hM3Dq*, to permit selective glial activation while imaging nociceptive nerve terminal activity in the gut with GCaMP. Consistent with our prior work characterizing the *GFAP::hM3Dq* glial chemogenetic line (17, 42), immunolabeling confirmed that hM3Dq receptor expression (HA tagged) was confined to glial processes and cell bodies co-labeled with GFAP (Fig. 8A). Further, the hM3Dq agonist clozapine-N-oxide (CNO) stimulated Ca^{2+} responses in enteric glia in whole-mount preparations loaded with the Ca^{2+} indicator dye Fluo-4 (fig. S5).

Our initial studies with this model were directed at determining whether specifically activating glia without the potential confounds of agonists on surrounding cells would produce similar effects on nociceptor sensitivity (Fig. 8B). As was the case with ADP, activation of enteric glia with CNO did not induce Ca^{2+} responses in $TRPV1^+$ nociceptors and did not alter capsaicin responses under baseline conditions (Fig. 8, C and D). However, in the presence of IL-1β, activating enteric glia with CNO resulted in a clear potentiation of nociceptor capsaicin responses (Fig. 8, C and E). Therefore, glial activation alone is sufficient to sensitize nociceptive afferents during inflammation. Similar to our findings using ADP as a glial agonist, blocking Cx43 with 43Gap26 inhibited the sensitization of nociceptors elicited by glial activation with CNO (Fig. 8, C and E). Likewise, blocking nociceptor EP_4 receptors with the selective antagonist L-161,982 inhibited the sensitization of nociceptors induced by glial activity (Fig. 8, C and E). Therefore, glial activity driven by chemogenetic Gq GPCRs sensitizes $TRPV1^+$ nociceptors in the context of inflammation through glial Cx43-dependent PGE_2 release, which acts on EP_4 receptors.

The in vitro experiments above show that acute exposure to IL-1β increases nociceptor sensitivity through glial mechanisms. To determine whether these mechanisms are relevant to nociceptor sensitization following colitis in vivo, we repeated the experiments in samples obtained from *Trpv1*$^{Cre;GCaMP5gtdT}$*;GFAP-hM3Dq* mice one week after DNBS colitis. Nociceptor responses to capsaicin were increased by approximately 10% following colitis; however, this did not reach statistical significance (Fig. 8, C and F). Similar to samples treated with IL-1β, stimulating enteric glia in samples obtained from animals that experienced colitis significantly increased capsaicin responses in TRPV1$^+$ nociceptors in an EP_4 receptor-dependent manner (Fig. 8, C and F). Nociceptor activity was also observed in these samples in response to stimulating enteric glia with CNO prior to their direct activation by capsaicin (Fig. 8F). This effect was not observed in preparations where glial stimulation was absent and in preparations where EP_4 receptors were blocked. Together these data show that enteric glia sensitize TRPV1$^+$ receptors during active inflammation and following the resolution of colitis in vivo.

Visceral hypersensitivity driven by IL-1β requires glial Cx43-mediated signaling in vivo

To test whether local glial-mediated sensitization contributes to broader pain behaviors in vivo, we assessed visceromotor responses (VMRs) to colorectal distensions in mice using non-invasive pressure recordings (20, 43, 44). This technique has been validated in multiple prior studies and eliminates the potential confounding factor of the surgery required for electromyography (EMG) recordings which can sensitize nociceptors and change enteric glial phenotype (20, 43). IL-1β had no effect on VMRs elicited in response to non-noxious or noxious distension pressures in males (Fig. 9A); however, female mice exhibited larger VMRs in response to a normally non-noxious distension pressure of 20mmHg following an enema of IL-1β (Fig. 9B). This suggests that females are more sensitive to developing allodynia following acute inflammation driven by IL-1β and supports the concept that sensitization of high-threshold nerves innervating the myenteric plexus are responsible for the effect. In line with our cellular imaging studies, baseline visceral sensitivity did not require glial Cx43 signaling and was not different between controls and animals lacking glial Cx43 (*Sox10*^{CreERT2}*;Cx43*$^{f/f}$) (Fig. 9C, D). In contrast, ablating glial Cx43 abolished the sensitizing effect of IL-1β on VMRs in females without changing responses in males (Fig. 9C, D). No significant changes in colonic compliance were observed between strains or IL-1β and control animals (fig. S6, A to D). Therefore, glial intercellular communication mediated by Cx43 contributes to visceral hypersensitivity during inflammation in a potentially sex-dependent manner.

DISCUSSION

Treating visceral pain is complicated by an unsatisfactory understanding of the causal mechanisms. Here, we show that enteric glia sensitize intestinal nociceptors through intercellular signaling mechanisms provoked by inflammation. Our approach allowed us to study events that sensitize sensory transduction in the gut and determine that normal glial signaling does not impact nociceptor sensitivity in health but plays a major role in sensitizing afferents during inflammation. The underlying mechanisms involve facilitating effects of proinflammatory cytokines on glial Cx43 hemichannels, an upregulation of glial

COX-2, and an increase in stimulated glial PGE_2 release which acts on EP_4 receptors. These glial mechanisms offer insight into mechanisms that promote visceral pain at the site of transduction.

Astrocytes and microglia modulate information in ascending pain pathways, contribute to the transition from acute to chronic pain, and are active in all forms of pain (21, 45). Here, we show that enteric glia share these properties at the most distant peripheral terminals of afferent neurons innervating the gut. Enteric glia, particularly those associated with neurons in the myenteric plexus, share some functional properties with astrocytes that might suggest similar roles in pain transmission. Sequencing data support this idea by showing that enteric glia upregulate genes associated with sensory transduction during inflammation (2) that are linked with downstream mechanisms in colon-projecting dorsal root ganglion (DRG) neurons (23). We have extended this link by showing a direct, functional interaction between enteric glia and nociceptors that sensitizes afferent transduction. This emerging theme suggests that glia present at all sites along ascending and descending pain pathways influence visceral perception.

Enteric glia gain functions that sensitize $TRPV1^+$ nociceptors under proinflammatory conditions, but apparently have little influence on nociceptor sensitivity in health. One interpretation of this difference is that enteric glia are normally under tonic inhibition that is released during inflammation. This possibility has been proposed for the nitrergic system, which is impaired following gut inflammation (26, 46). Alternatively, the gain of glial function during inflammation could reflect a protective response that prevents further damage. Although these possibilities are not exclusive, the former seems most likely given the observed upregulation of proinflammatory genes, increased secretory capacity through Cx43, and acute effects on nerve fibers (20, 47).

Our results agree with prior work showing that enteric glia produce and release PGE_2 during inflammation (34). PGE_2 is a mediator of pain that sensitizes $TRPV1^+$ nociceptors (35) and promotes enteric neuroplasticity, enteric neuron hyperexcitability, and dysmotility in models of colitis (36). Many of the changes to both intrinsic and extrinsic neurons during inflammation could be attributed to glial PGE_2 production. Other cell types do contribute to the available pool of PGE_2 and mast cell-derived PGE_2 is considered important in visceral hypersensitivity (10). However, mast cell numbers in IBS are inconsistent (11), decrease in frequency from the cecum to rectum (12), and where present, are mainly associated with mucosal afferents (13–15). Neutrophils, also contribute to PGE_2 during colitis; however, neutrophil infiltration occurs within the first 12h following the induction of colitis (38) and most neutrophils are located in the mucosa (48, 49). Mucosal afferents comprise about 10% of colon-innervating afferent terminals and display low activation thresholds, which if further sensitized could contribute to hyperalgesia but would not cause a major shift in visceral sensitivity. Spinal afferents innervating deeper layers such as the circular muscle and myenteric ganglia (14) exhibit high activation thresholds and sensitizing mechanisms that decrease their activation thresholds would cause a major shift in sensory signaling associated with allodynia (13). Glia, immune cells, and epithelial cells likely have complementary compartmentalized roles in visceral hypersensitivity (50, 51); however, glial mechanisms appear dominant in the myenteric plexus where their sensitizing effects on

TRPV1$^+$ nociceptors involve the actions of PGE_2 on EP4 receptors. Multiple prostaglandins receptors contribute to pain sensitization (35, 52, 53) and expressed by enteric neurons, immune cells, and other cell types that could also contribute to the mechanisms observed in this study (54).

The effects of IL-1β and glial signaling on visceral pain were sexually dimorphic with a prominent role in females. Sexual dimorphism in pain mechanisms is well known (55, 56) and the nature of the pain-producing insult impacts males and females differentially, in part due to greater proinflammatory responses in females than males. Cytokine expression showed that females exhibited greater increases in most cytokines during colitis, but similar glial mechanisms may be active in both sexes and evoked with sufficient cytokine concentrations. This could explain why sex differences were not observed *in vitro* when cells were exposed to equivalent cytokine concentrations. Another possibility is that female mice are more sensitive to PGE_2, which is supported by gene expression data showing that prostaglandin signaling is enriched in DRG neurons in female mice and findings showing that PGE_2 produces greater effects on mechanical allodynia in females (56). This suggests that PGE_2 pain thresholds are lower in females, which could explain the observed differences in our VMR data.

Our study identifies enteric glial signaling as a mechanism that promotes visceral hypersensitivity at the initial site of sensory transduction. Inflammation-induced changes in enteric glia increase their potential to modulate surrounding cells through effects on glial transmitter synthesis and release mechanisms. Perturbing these glial mechanisms limits visceral sensitization. Nonsteroidal anti-inflammatory drugs (NSAIDs) are the most frequently used analgesics that suppress inflammatory pain by inhibiting COX-1 and/or COX-2 and reducing the production of prostanoids (35). However, products of COX-2 activity, such as PGE_2, are involved in diverse physiological processes and current drugs have serious side effects (57). Cell-specific therapies targeting glial mechanisms could avoid these side effects and represent an important step forward in limiting visceral pain at its source.

MATERIALS AND METHODS

Chemicals and Reagents

Chemicals and reagents were purchased from Millipore Sigma unless otherwise stated below.

Animals—All work involving animals was conducted in accordance with the National Institutes of Health (NIH) *Guide for Care and Use of Laboratory Animals*, ARRIVE guidelines and was approved by the Institutional Animal Care and Use Committee (IACUC) at Michigan State University (AUF# PROTO202100150). An equal number of 14–16 weeks male and female mice with *C57BL/6* background were used for all experiments unless otherwise stated. All mice were maintained on a 12h:12h light-dark cycle in a temperature-controlled environment with access to food (Diet Number 2919; Envigo, Indianapolis, IN) and water ad libitum.

Transgenic mice expressing the genetically encoded calcium indicator GCaMP5g in sensory neurons (*Trpv1*$^{Cre;GCaMP5g\text{-}tdT}$) were bred in-house and were generated by crossing *B6.129-Trpv1*$^{tm1[cre]Bbm/J}$ mice [TRPV1Cre (017769; RRID: IMSR_JAX:017769; Jackson Laboratory)] with *Polr2a*$^{tm1(CAG\text{-}GcaMP5g,\text{-}tdTomato)Tvrd}$ (RRID: IMSR_ JAX:024477) mice (2). These mice were crossed with *GFAP-hM3Dq* (MGI:6148045; gifted by Dr. Ken McCarthy; University of North Carolina at Chapel Hill) (17) and were bred for experiments as heterozygotes to produce *Trpv1*$^{Cre;GcaMP5gtdT}$*;GFAP-hM3Dq* mice. Mice with a tamoxifen-sensitive deletion of the gene encoding Cx43 (*Gja1*) in enteric glia (*Sox10*^{creERT2}*;Cx43*$^{f/f}$) were also bred in-house and generated as previously described (30) by crossing *Sox10*^{CreERT2} (MGI:5910373; gifted by Dr. Vassilis Pachnis, The Francis Crick Institute, London, UK) mice with *Gja1*^{tm1Dlg} mice [Cx43f/f (008039; RRID: IMSR_JAX:008039; Jackson Laboratory)]. Cre^{ERT2} activity was induced in by feeding the animals with chow containing tamoxifen citrate (400mg/kg, TD.14084; Envigo) for 2 weeks followed by 1 week of normal chow before use. Double- and Triple-transgenic mice were maintained as hemizygous for Cre (*Trpv1*^{Cre} *or Sox10*^{CreERT2}) and homozygous for the floxed allele (*Polr2a*$^{tm1(CAG\text{-}GcaMP5g,\text{-}tdTomato)Tvrd}$ or *Cx43*$^{f/f}$). Genotyping was performed by the Research Technology Support Facility Genomics Core at MSU and Transnetyx (Cordova, TN).

In vivo model of colitis—Colitis was induced in male and female mice under isoflurane anesthesia by an 0.1 mL enema of 40 to 55 ug/mL of di-nitro benzenesulfonic acid (DNBS; 150959, MP Biomedicals/556971, Sigma) dissolved in 30–50% ethanol (31). Control animals received 0.9% saline enema. Mice were monitored closely and weighed daily and sacrificed at 6 hours, 48 hours, 1 week, or 3 weeks following DNBS. Macroscopic damage was assessed as previously described (26, 31) at 6 and 48 hours and three weeks to evaluate the degree of inflammation and recovery. The presence of fecal blood, diarrhea, and/or hemorrhage received one point per feature present. Adhesion of the colon to other organs and peritoneal space was scored 0, 1, or 2 based on the severity of adhesions. Colon length and thickness were also scored with greater points for a shortened and/or thickened colon.

Multiplex Cytokine Assay—Whole colon samples were collected from control and DNBS treated mice at 6 hours, 48 hours, and 3 weeks. Tissue was processed for multiplex immunoassay as previously described (58). Colonic samples were homogenized in a Tris-buffered saline Tween buffer solution to extract protein. After, homogenates were centrifuged at 10,000*g* for 10 minutes at 4°C. Cytokine and chemokine levels were evaluated using bead-based multiplex immunoassays provided and performed by Eve Technologies (Calgary, AB, Canada).

Glial permeability assay—Glial Cx43 hemichannel activity was measured by ethidium bromide (EtBr) dye uptake as previously described (28, 59). Live whole-mount longitudinal muscle-myenteric plexus (LMMP) preparations were dissected from from the distal colon in 35mm^2 sylgard-coated dishes and treated with an enzyme mix containing 1 U/mL Dispase (17105–041, Gibco) and 150 U/mL of Collagenase Type II (17101–015, Gibco) for 15 minutes at room temperature. Preparations were incubated for 30 minutes at 37°C in 5% CO_2/95% air in either DMEM/F-12 (11039047, Thermofisher)

media only (Control) or interleukin 1-β (IL1-β, 10ng/mL; 401-ML-005, R&D Systems), interleukin-6 (IL-6, 10ng/mL; 406-ML-005, R&D Systems), interferon-γ (IFN-γ, 10ng/mL, BMS326, Invitrogen), tumor necrosis factor-α (TNFα, 10ng/mL; 315–01A, PeproTech), interleukin-17 (IL-17, 10ng/mL; ab9567, Abcam) in the presence or absence of mimetic peptide antagonists for Cx43 (43Gap26, 100 μM; 62644, Anaspec, Inc.) or pannexin-1 (10Panx, 300 μM; 61911, Anaspec Inc.), and the pore blocker gadolinium (Gd, 25 μM; G7532, Sigma). After, the mixture was removed and preparations were incubated with ethidium bromide (EtBr; 5 μM; 15585–011, Invitrogen) in the presence or absence of the purinergic agonist ADP (100 μM; A5285, Sigma) for 10 minutes at 37°C. Extracellular EtBr was removed by three washes in fresh DMEM. EtBr fluorescence was immediately recorded using an upright Olympus BX51WI fixed-stage microscope fitted with a 40X water-immersion objective (LUMPlan N, 0.8 n.a.) and a Lambda DG-4 Plus xenon light source (Sutter). Ganglia were identified based on morphological features defined in previous work and acquired using MetaMorph Software (Molecular Devices).

Immunohistochemistry—Preparations of mouse colonic myenteric plexus prepared from segments of healthy or 48h post-DNBS intestines preserved in Zamboni's fixative or 4% PFA overnight at 4°C or 2h at room temperature and were processed for whole-mount immunohistochemistry or frozen cross sections as previously described (20, 31). LMMP whole-mounts or frozen slides were rinsed 3 times for 10 minutes each with 0.1% Triton X-100 in PBS (PBSTriton) followed by a 45-minute incubation in blocking solution (4% normal goat or normal donkey serum, 0.4% Triton X-100, and 1% bovine serum albumin). Preparations were incubated with primary antibodies overnight at room temperature and secondary antibodies for 2 hours at room temperature before mounting (table S1).

Fluorescence in situ hybridization (RNAscope)—LMMP tissue preparations from distal colon were collected from control and DNBS mice 48h after treatment. Samples were generated following the fixation and dissection procedures described above. RNAscope was performed using the Advanced Cell diagnostics (ACD) RNAscope 2.5 HD HD Assay-RED reported elsewhere (60). Tissues were dehydrated and subsequently rehydrated by a serial ethanol gradient (25%, 50%, 75%, 100% in PBS with 0.1% Triton X-100) prior to H2O2 treatment. Tissues were then digested with Protease III for 45 minutes and incubated with a probe for *Ptgs2* (table S1). Tissues were washed 3 times for 5 minutes between each step with PBS (before probe incubation) or with RNAscope™ wash buffer (between amplification steps). Labeling was confirmed with species-specific positive and negative controls. Immunohistochemistry was performed following completion of the RNAscope protocol as described above.

Imaging—Immunohistochemistry and RNAscope fluorescent labeling was evaluated using the 20 or 40x objective (0.75 numerical aperture, Plan Fluor; Nikon) of an upright epifluorescence microscope (Nikon Eclipse Ni) with a Retiga 2000R camera (Qimaging) controlled by Qcapture Pro 7.0 (Qimaging) software. Representative images were acquired through the 60x-oil immersion objective (PlanApochromat, 1.42 numerical aperture) of an inverted Fluoview FV1000 confocal microscope (Olympus) or Zeiss LSM 880 NLO

confocal system (Zeiss) using Zen Black software and a 20x objective (0.8 numerical aperture, Plan ApoChromat; Zeiss).

Glial PGE_2 release—PGE_2 was measured in supernatants collected from cultures of primary enteric glia. Enteric glia were isolated from male and female wild-type mice and cultured using a modification of protocols previously described (20). Whole colons were cut in small 2–3 cm segments and rod-dissected in DMEM-F12 to remove the myenteric plexus and longitudinal muscle layers and were digested in 2.5 mL of HBSS/HEPES buffer (14064, Gibco) containing Liberase TH (12.5 μg/mL; 5401119001, Sigma) and Dnase I (100 Kuntz units/ml; D5025–15KU, Sigma) for 30 minutes at 37°C. Cell suspensions were spun down (5 min at 1000x*g* and 4°C) and resuspended in 2 ml of complete medium made up of DMEM/Nutrient Mixture F-12 (11330–032, Thermofisher) containing phenol red supplemented with L-glutamine and HEPES (H3375, Sigma), penicillin and streptomycin (100 U/ml and 100μg/ml; 15140122, Gibco), and 10% fetal bovine serum (FBS, Denville Scientific, Inc.). Cells were plated in 24 well plates on coverslips coated with poly D-Lysine (100μg/ml, A-003-E, Sigma). Cell suspensions were initially seeded in the complete medium and plates were placed in an incubator (37C, 95% O_2 / 5% CO_2). New media composed of DMEM/Nutrient Mixture F-12 containing phenol red supplemented with L-glutamine and HEPES and substituted with antibiotics (penicillin 100 U/mL and streptomycin 100 mg/mL), GIBCO N-2 Supplement (0.2%; 17502048), GIBCO G-5 Supplement (0.2%; 17503012) and mouse NGF-β (0.05%; GFM11–20, Cells GS) was exchanged every 2 days. Experiments were performed once cells reached 50%–80% confluency (1–2 weeks). Cells were treated with IL-1β (10ng/mL) or media for 1 hour and stimulated with ADP (100μM) for 10 minutes. In some cases, Cx43 activity was blocked with 43Gap26 (100 μM) for 10 minutes prior to stimulation. After, supernatants were collected and cells were fixed in 4% PFA for 30 minutes. PGE_2 release was quantified using PGE_2 ELISA kit (KGE004B, R&D Systems). Culture purity was evaluated with IHC for GFAP, peripherin, and α-smooth muscle actin (table S1) and considered for analysis if above a 90% ratio of glia. All experimental groups were run in duplicate and averaged for statistical analysis. Two technical replicates were run per experimental group.

Ca^{2+} imaging—Live whole-mounts of colon myenteric plexus from either *$Trpv1^{Cre;GCaMP5g\text{-}tdT}$ or $Trpv1^{Cre;GCaMP5gtdT}$;GFAP-hM3Dq* from control or DNBS (post 1wk) mice were prepared for Ca^{2+} imaging as previously described (17). Whole-mount circular muscle-myenteric plexus (CMMP) preparations were microdissected from mouse colons were continuously superfused with fresh, prewarmed (37°C) Kreb's buffer consisting of (in mM): 121 NaCl, 5.9 KCl, 2.5 CaCl2, 1.2 MgCl2, 1.2 NaH2PO4, 10 HEPES, 21.2 NaHCO3, 1 pyruvic acid, and 8 glucose (pH adjusted to 7.4 with NaOH) at a flow rate of 2–3 mL min-1. Preparations were incubated for 30min with or without IL-1β (10 μg/mL) and either 43Gap26 (100 μM) or L-161,982 (50μM; 10011565, Cayman Chemical) to disrupt the release of glial mediators through Cx43 and inhibit EP_4 receptors on nociceptors. CNO (10 μM; National Institute on Drug Abuse Drug Supply Program at the National institute of Health), ADP (100μM), and capsaicin (3 μM; 360376, Sigma) were applied for 30 seconds to activate glia and TRPV1 positive nociceptors, respectively. hM3Dq receptor expression in glia was validated by with Fluo-4 AM. Fluo-4 was loaded in the dark with Pluronic F-127

and 200mmol/L probenecid (P36400, Invitrogen) in DMEM/F-12. Images were acquired every second through 40x water-immersion objective (LUMPlanFI, 0.8 numerical aperture) of an upright Olympus BX51WI fixed stage microscope (Olympus, Tokyo, Japan) using NIS-Elements software (v.4.5; Nikon, Tokyo, Japan) and an Andor Zyla sCMOS camera (Oxford Instruments, Abingdon, United Kingdom). To obtain higher spatial and temporal resolution of Ca^{2+} responses during validation of our genetic models, representative videos were obtained using a Nikon A1R HD25 confocal spinning-disk microscope (Nikon, Tokyo, Japan). Whole-mounts were superfused with Krebs buffer, (37°C) at 2–3 mL/min. To obtain higher spatial and temporal resolution of Ca^{2+} responses during validation of our genetic models, representative videos were obtained using a Nikon A1R HD25 confocal spinning-disk microscope (Nikon, Tokyo, Japan). In these cases, tissues were imaged through a 20x Nikon objective lens (CFI Apochromat LWD Lambda20xC WI, 0.95 numerical aperture). Confocal images were captured using a Nikon DS-Ri2 digital camera (Nikon, Tokyo, Japan) and recorded using NIS-Elements C software (Nikon).

In vivo assessment of visceral sensitivity—Visceral sensitivity was measured as previously described by non-invasive assessment of visceromotor responses VMRs to colorectal distensions (20, 43). Intracolonic pressure was measured by a miniaturized pressure transducer catheter (SPR-524, Mikro-Tip catheter, Millar Instruments) equipped with a custom-made plastic balloon. Mice were trained to restrainers for 3 hours one day prior to the experiment. Mice received an enema of 0.9% saline or IL-1β (100ng/mL) and following 3 hours were briefly anesthetized with isoflurane while the pressure transducer-balloon was inserted into the colorectum. Mice were then acclimated to restraints for 30 minutes before starting the colorectal distension procedure. Graded phasic distensions (20, 40, 60, and 80 mmHg, 2 times each, 20 second duration, 3-minute interstimulus interval) were delivered to the balloon by a barostat (G&J Electronics) and VMR recordings were acquired using LabChart 8 (AD instruments). VMR recordings were performed as repeated measures experiments where control recordings were performed one week prior to conducting experiments with IL-1β.

Analysis and Statistics—Sample size was determined using a priori power analysis (G*Power 3.1) assuming 80% power with a desired significance level of 0.05 and anticipating medium effect sizes (f = 1.0) based on previous experience and similar studies described in the literature. Male and female mice were analyzed separately and pooled if lacking statistical differences. Supplemental table 2 summarizes statistical analysis for sex differences. Whole animals were considered as individual n's for immunoassay, immunohistochemistry, culture experiments, *in situ* hybridization, and *in vivo* analysis. Outliers were identified with a Grubbs' test (alpha = 0.05) and removed for statistical analysis. Averaged ganglionic cellular responses from multiple mice represented n's for Ca^{2+} imaging and dye uptake experiments. Immunolabeling data were analyzed in FIJI (National Institutes of Health) either by calculating arbitrary mean fluorescence values per ganglionic area or by manually counting positively labeled cells and normalizing by area. Dye uptake experiments considered average glial fluorescence values per ganglion and each experiment was normalized to the control mean of the day. Ca^{2+} imaging traces represent the average change in fluorescence over time of the mean number of individual afferents per

preparation. Individual nerve fibers were identified by tdTomato expression and morphology (61) and mean fluorescence was quantified using SparkAn (Dr. Adrian Bonev, University of Vermont) or NIS-Elements Analysis software. Ca^{2+} recordings were motion corrected using the ND Processing function in NIS-Elements software. Raw VMR traces were processed by running the SmoothSec and root mean square functions in LabChart 8 software to filter phasic colonic contractions (20). Following filtering the integral from the response at each distension pressure and the baseline mean from 20 seconds prior to the distension were obtained. Responses were considered significant if they were at least 2 SDV above the baseline mean. Data were analyzed using Students' t-test, one-way or two-way ANOVA using Graphpad 9 software (Prism) and are presented as mean ± standard error of the mean (SEM).

Supplementary Material

Refer to Web version on PubMed Central for supplementary material.

Acknowledgements:

We thank Jonathon McClain for technical support and animal care.

Funding:

BDG receives support from grants R01DK103723 and R01DK120862 from the National Institute of Diabetes and Digestive and Kidney Diseases (NIDDK) of the National Institutes of Health (NIH). WMS is the recipient of an NRSA Award from the NIDDK (F31DK127732). The content is solely the responsibility of the Authors and does not necessarily represent the official views of the NIH.

Data and Materials Availability:

The multiplex immune assay data have been deposited to Dryad, DOI: 10.5061/dryad.jwstqjqgr. All other data needed to evaluate the conclusions in the paper are present in the paper or the Supplementary Materials.

REFERENCES and NOTES

1. Peery AF, Crockett SD, Barritt AS, Dellon ES, Eluri S, Gangarosa LM, Jensen ET, Lund JL, Pasricha S, Runge T, Schmidt M, Shaheen NJ, Sandler RS, Burden of Gastrointestinal, Liver, and Pancreatic Diseases in the United States. Gastroenterology. 149, 1731–1741.e3 (2015). [PubMed: 26327134]
2. Delvalle NM, Dharshika C, Morales-Soto W, Fried DE, Gaudette L, Gulbransen BD, Communication between enteric neurons, glia, and nociceptors underlies the effects of tachykinins on neuroinflammation. Cellular and Molecular Gastroenterology and Hepatology, 321–344 (2018). [PubMed: 30116771]
3. Stein C, Machelska H, Modulation of Peripheral Sensory Neurons by the Immune System: Implications for Pain Therapy. Pharmacological Reviews. 63, 860–881 (2011). [PubMed: 21969325]
4. Simrén M, Törnblom H, Palsson OS, van Tilburg MA, Oudenhove L, Tack J, Whitehead WE, Visceral hypersensitivity is associated with GI symptom severity in functional GI disorders: consistent findings from five different patient cohorts. Gut. 67, 255–262 (2018). [PubMed: 28104632]
5. Klem F, Wadhwa A, Prokop LJ, Sundt WJ, Farrugia G, Camilleri M, Singh S, Grover M, Prevalence, Risk Factors, and Outcomes of Irritable Bowel Syndrome After Infectious Enteritis:

A Systematic Review and Meta-analysis. Gastroenterology. 152, 1042–1054.e1 (2017). [PubMed: 28069350]

6. Spiller R, Major G, IBS and IBD — separate entities or on a spectrum? Nat Rev Gastroentero. 13, 613–621 (2016).
7. Mayer EA, Tillisch K, The Brain-Gut Axis in Abdominal Pain Syndromes. Annual Review of Medicine. 62, 381–396 (2011).
8. Kyloh M, Nicholas S, Zagorodnyuk VP, Brookes SJ, Spencer NJ, Identification of the Visceral Pain Pathway Activated by Noxious Colorectal Distension in Mice. Frontiers in Neuroscience. 5, 16 (2011). [PubMed: 21390285]
9. Esquerre N, Basso L, Defaye M, Vicentini FA, Cluny N, Bihan D, Hirota SA, Schick A, Jijon HB, Lewis IA, Geuking MB, Sharkey KA, Altier C, Nasser Y, Colitis-Induced Microbial Perturbation Promotes Postinflammatory Visceral Hypersensitivity. Cell Mol Gastroenterology Hepatology. 10, 225–244 (2020).
10. Grabauskas G, Wu X, Gao J, Li J-Y, Turgeon DK, Owyang C, Prostaglandin E2, Produced by Mast Cells in Colon Tissues from Patients with Irritable Bowel Syndrome, Contributes to Visceral Hypersensitivity in Mice. Gastroenterology. 158, 2195–2207 (2020). [PubMed: 32084424]
11. Bashashati M, Moossavi S, Cremon C, Barbaro MR, Moraveji S, Talmon G, Rezaei N, Hughes PA, Bian ZX, Choi CH, Lee OY, Coëffier M, Chang L, Ohman L, Schmulson MJ, McCallum RW, Simren M, Sharkey KA, Barbara G, Colonic immune cells in irritable bowel syndrome: A systematic review and meta-analysis. Neurogastroenterol Motil. 30, e13192 (2018).
12. Hasler WL, Grabauskas G, Singh P, Owyang C, Mast cell mediation of visceral sensation and permeability in irritable bowel syndrome. Neurogastroenterol Motil. 34, e14339 (2022). [PubMed: 35315179]
13. Grundy L, Erickson A, Brierley SM, Visceral Pain. Annu Rev Physiol. 81, 1–24 (2018). [PubMed: 30256725]
14. Spencer NJ, Kyloh M, Duffield M, Identification of Different Types of Spinal Afferent Nerve Endings That Encode Noxious and Innocuous Stimuli in the Large Intestine Using a Novel Anterograde Tracing Technique. Plos One. 9, e112466 (2014). [PubMed: 25383884]
15. Schemann M, Camilleri M, Functions and Imaging of Mast Cell and Neural Axis of the Gut. Gastroenterology. 144, 698–704.e4 (2013). [PubMed: 23354018]
16. Morales-Soto W, Gulbransen BD, Enteric glia: a new player in abdominal pain. Cell Mol Gastroenterology Hepatology. 7, 433–445 (2018).
17. McClain JL, Fried DE, Gulbransen BD, Agonist-Evoked Ca2+ Signaling in Enteric Glia Drives Neural Programs That Regulate Intestinal Motility in Mice. Cell Mol Gastroenterology Hepatology. 1, 631–645 (2015).
18. Grubišić V, Verkhratsky A, Zorec R, Parpura V, Enteric glia regulate gut motility in health and disease. Brain Res Bull. 136, 109–117 (2018). [PubMed: 28363846]
19. Chow AK, Grubišić V, Gulbransen BD, Enteric Glia Regulate Lymphocyte Activation via Autophagy-Mediated MHC-II Expression. Cell Mol Gastroenterology Hepatology. 12, 1215–1237 (2021).
20. Grubišić V, McClain JL, Fried DE, Grants I, Rajasekhar P, Csizmadia E, Ajijola OA, Watson RE, Poole DP, Robson SC, Christofi FL, Gulbransen BD, Enteric Glia Modulate Macrophage Phenotype and Visceral Sensitivity following Inflammation. Cell Reports. 32, 108100 (2020). [PubMed: 32905782]
21. Ji R-R, Chamessian A, Zhang Y-Q, Pain regulation by non-neuronal cells and inflammation. Science. 354, 572–577 (2016). [PubMed: 27811267]
22. Chen MJ, Kress B, Han X, Moll K, Peng W, Ji R, Nedergaard M, Astrocytic CX43 hemichannels and gap junctions play a crucial role in development of chronic neuropathic pain following spinal cord injury. Glia. 60, 1660–1670 (2012). [PubMed: 22951907]
23. Wangzhou A, Paige C, Neerukonda SV, Naik DK, Kume M, David ET, Dussor G, Ray PR, Price TJ, A ligand-receptor interactome platform for discovery of pain mechanisms and therapeutic targets. Sci Signal. 14, 1–21 (2021).
24. Neurath MF, Cytokines in inflammatory bowel disease. Nat Rev Immunol. 14, 329–342 (2014). [PubMed: 24751956]

25. Johnson AC, Farmer AD, Ness TJ, Meerveld BG-V, Critical evaluation of animal models of visceral pain for therapeutics development: A focus on irritable bowel syndrome. Neurogastroenterol Motil Official J European Gastrointest Motil Soc. 32, e13776 (2019).
26. Brown IAM, McClain JL, Watson RE, Patel BA, Gulbransen BD, Enteric Glia Mediate Neuron Death in Colitis Through Purinergic Pathways That Require Connexin-43 and Nitric Oxide. Cmgh Cell Mol Gastroenterology Hepatology. 2, 77–91 (2016).
27. Korolkova OY, Myers JN, Pellom ST, Wang L, M'koma AE, Characterization of Serum Cytokine Profile in Predominantly Colonic Inflammatory Bowel Disease to Delineate Ulcerative and Crohn's Colitides. Clin Medicine Insights Gastroenterology. 8, 29–44 (2015). [PubMed: 26078592]
28. McClain JL, Gulbransen BD, The acute inhibition of enteric glial metabolism with fluoroacetate alters calcium signaling, hemichannel function, and the expression of key proteins. Journal of Neurophysiology. 117, 365–375 (2017). [PubMed: 27784805]
29. Orellana JA, Sáez PJ, Shoji KF, Schalper KA, Palacios–Prado N, Velarde V, Giaume C, Bennett M, Sáez JC, Modulation of Brain Hemichannels and Gap Junction Channels by Pro-Inflammatory Agents and Their Possible Role in Neurodegeneration. Antioxidants & Redox Signaling. 11, 369–399 (2009). [PubMed: 18816186]
30. Grubišić V, Gulbransen BD, Enteric glial activity regulates secretomotor function in the mouse colon but does not acutely affect gut permeability. The Journal of Physiology. 595, 3409–3424 (2017). [PubMed: 28066889]
31. Gulbransen BD, Bashashati M, Hirota SA, Gui X, Roberts JA, MacDonald JA, Muruve DA, McKay DM, Beck PL, Mawe GM, Thompson RJ, Sharkey KA, Activation of neuronal P2X7 receptor–pannexin-1 mediates death of enteric neurons during colitis. Nat Med. 18, 600–604 (2012). [PubMed: 22426419]
32. Balemans D, Mondelaers S, Cibert-Goton V, Stakenborg N, Aguilera-Lizarraga J, Dooley J, Liston A, Bulmer D, Berghe VP, Boeckxstaens G, Wouters M, Evidence for long-term sensitization of the bowel in patients with post-infectious-IBS. Scientific reports. 7, 13606 (2017). [PubMed: 29051514]
33. Lai NY, Musser MA, Pinho-Ribeiro FA, Baral P, Jacobson A, Ma P, Potts DE, Chen Z, Paik D, Soualhi S, Yan Y, Misra A, Goldstein K, Lagomarsino VN, Nordstrom A, Sivanathan KN, Wallrapp A, Kuchroo VK, Nowarski R, Starnbach MN, Shi H, Surana NK, An D, Wu C, Huh JR, Rao M, Chiu IM, Gut-Innervating Nociceptor Neurons Regulate Peyer's Patch Microfold Cells and SFB Levels to Mediate Salmonella Host Defense. Cell. 180, 33–49.e22 (2020). [PubMed: 31813624]
34. Valès S, Bacola G, Biraud M, Touvron M, Bessard A, Geraldo F, Dougherty KA, Lashani S, Bossard C, Flamant M, Duchalais E, Marionneau-Lambot S, Oullier T, Oliver L, Neunlist M, Vallette FM, Landeghem LV, Tumor cells hijack enteric glia to activate colon cancer stem cells and stimulate tumorigenesis. Ebiomedicine. 49, 172–188 (2019). [PubMed: 31662289]
35. Kawabata A, Prostaglandin E2 and Pain—An Update. Biol Pharm Bull. 34, 1170–1173 (2011). [PubMed: 21804201]
36. Linden DR, Sharkey KA, Ho W, Mawe GM, Cyclooxygenase-2 contributes to dysmotility and enhanced excitability of myenteric AH neurones in the inflamed guinea pig distal colon. J Physiology. 557, 191–205 (2004).
37. McClain JL, Mazzotta EA, Maradiaga N, Duque-Wilckens N, Grants I, Robison AJ, Christofi FL, Moeser AJ, Gulbransen BD, Histamine-dependent interactions between mast cells, glia, and neurons are altered following early-life adversity in mice and humans. Am J Physiol-gastr L. 319, G655–G668 (2020).
38. Linden DR, Couvrette JM, Ciolino A, Mcquoid C, Blaszyk H, Sharkey KA, Mawe GM, Indiscriminate loss of myenteric neurones in the TNBS-inflamed guinea-pig distal colon. Neurogastroenterol Motil. 17, 751–760 (2005). [PubMed: 16185315]
39. Hockley JR, Tranter MM, McGuire C, Boundouki G, Cibert-Goton V, Thaha MA, Blackshaw AL, Michael GJ, Baker MD, Knowles CH, Winchester WJ, Bulmer DC, P2Y Receptors Sensitize Mouse and Human Colonic Nociceptors. The Journal of Neuroscience. 36, 2364–2376 (2016). [PubMed: 26911685]

40. Wood JD, The enteric purinergic P2Y1 receptor. Curr Opin Pharmacol. 6, 564–570 (2006). [PubMed: 16934527]
41. Gao Z-G, Ding Y, Jacobson KA, P2Y13 receptor is responsible for ADP-mediated degranulation in RBL-2H3 rat mast cells. Pharmacol Res. 62, 500–505 (2010). [PubMed: 20813187]
42. Ahmadzai MM, Seguella L, Gulbransen BD, Circuit-specific enteric glia regulate intestinal motor neurocircuits. P Natl Acad Sci Usa. 118, e2025938118 (2021).
43. Larauche M, Gourcerol G, Wang L, Pambukchian K, Brunnhuber S, Adelson DW, Rivier J, Million M, Taché Y, Cortagine, a CRF1 agonist, induces stresslike alterations of colonic function and visceral hypersensitivity in rodents primarily through peripheral pathways. Am J Physiology Gastrointest Liver Physiology. 297, G215–27 (2009).
44. Larauche M, Erchegyi J, Miller C, Sim MS, Rivier J, Behan D, Taché Y, Peripheral CRF-R1/CRF-R2 antagonist, astressin C, induces a long-lasting blockade of acute stress-related visceral pain in male and female rats. Peptides. 157, 170881 (2022). [PubMed: 36185037]
45. Defaye M, Abdullah NS, Iftinca M, Hassan A, Agosti F, Zhang Z, Cumenal M, Zamponi GW, Altier C, Gut-innervating TRPV1+ Neurons Drive Chronic Visceral Pain via Microglial P2Y12 Receptor. Cell Mol Gastroenterology Hepatology. 13, 977–999 (2022).
46. Smith TK, Koh SD, A model of the enteric neural circuitry underlying the generation of rhythmic motor patterns in the colon: the role of serotonin. Am J Physiol-gastr L. 312, G1–G14 (2017).
47. Froger N, Orellana JA, Calvo C-F, Amigou E, Kozoriz MG, Naus CC, Sáez JC, Giaume C, Inhibition of cytokine-induced connexin43 hemichannel activity in astrocytes is neuroprotective. Molecular and Cellular Neuroscience. 45, 37–46 (2010). [PubMed: 20684043]
48. van Lierop PPE, de Haar C, LindenberghKortleve DJ, SimonsOosterhuis Y, van Rijt LS, Lambrecht BN, Escher JC, Samsom JN, Nieuwenhuis EES, T‐cell regulation of neutrophil infiltrate at the early stages of a murine colitis model. Inflamm Bowel Dis. 16, 442–451 (2010). [PubMed: 19714763]
49. Venkataramana S, Lourenssen S, Miller KG, Blennerhassett MG, Early inflammatory damage to intestinal neurons occurs via inducible nitric oxide synthase. Neurobiol Dis. 75, 40–52 (2015). [PubMed: 25562655]
50. Aguilera-Lizarraga J, Hussein H, Boeckxstaens GE, Immune activation in irritable bowel syndrome: what is the evidence? Nat Rev Immunol, 1–13 (2022). [PubMed: 34799725]
51. Bayrer JR, Castro J, Venkataraman A, Touhara KK, Rossen ND, Morrie RD, Maddern J, Hendry A, Braverman KN, Garcia-Caraballo S, Schober G, Brizuela M, Navarro FMC, Bueno-Silva C, Ingraham HA, Brierley SM, Julius D, Gut enterochromaffin cells drive visceral pain and anxiety. Nature. 616, 137–142 (2023). [PubMed: 36949192]
52. Ma W, Li L, Xing S, PGE2/EP4 receptor and TRPV1 channel are involved in repeated restraint stress-induced prolongation of sensitization pain evoked by subsequent PGE2 challenge. Brain Res. 1721, 146335 (2019). [PubMed: 31302096]
53. Moriyama T, Higashi T, Togashi K, Iida T, Segi E, Sugimoto Y, Tominaga T, Narumiya S, Tominaga M, Sensitization of TRPV1 by EP1 and IP reveals peripheral nociceptive mechanism of prostaglandins. Mol Pain. 1, 3–3 (2005). [PubMed: 15813989]
54. Dey I, Lejeune M, Chadee K, Prostaglandin E2 receptor distribution and function in the gastrointestinal tract. Brit J Pharmacol. 149, 611–623 (2006). [PubMed: 17016496]
55. Prusator DK, Meerveld BG-V, Sex-related differences in pain behaviors following three early life stress paradigms. Biol Sex Differ. 7, 29 (2016). [PubMed: 27293543]
56. Tavares-Ferreira D, Ray PR, Sankaranarayanan I, Mejia GL, Wangzhou A, Shiers S, Uttarkar R, Megat S, Barragan-Iglesias P, Dussor G, Akopian AN, Price TJ, Sex Differences in Nociceptor Translatomes Contribute to Divergent Prostaglandin Signaling in Male and Female Mice. Biol Psychiat. 91, 129–140 (2022). [PubMed: 33309016]
57. Patrono C, Cardiovascular effects of cyclooxygenase-2 inhibitors: a mechanistic and clinical perspective. Brit J Clin Pharmaco. 82, 957–964 (2016).
58. Hernandez S, Fried DE, Grubišić V, McClain JL, Gulbransen BD, Faseb J, in press, doi:10.1096/fj.201802572r.
59. Orellana JA, Hernández DE, Ezan P, Velarde V, Bennett MVL, Giaume C, Sáez JC, Hypoxia in high glucose followed by reoxygenation in normal glucose reduces the viability of cortical

astrocytes through increased permeability of connexin 43 hemichannels. Glia. 58, 329–343 (2010). [PubMed: 19705457]

60. Ahmadzai MM, McClain JL, Dharshika C, Seguella L, Giancola F, Giorgio RD, Gulbransen BD, LPAR1 regulates enteric nervous system function through glial signaling and contributes to chronic intestinal pseudo-obstruction. J Clin Investigation. 132, e149464 (2022).
61. Spencer NJ, Magnúsdóttir EI, Jakobsson JE, Kestell G, Chen BN, Morris D, Brookes SJ, Lagerström MC, CGRPα within the Trpv1-Cre population contributes to visceral nociception. American journal of physiology. Gastrointestinal and liver physiology. 314, G188–G200 (2018). [PubMed: 28971837]

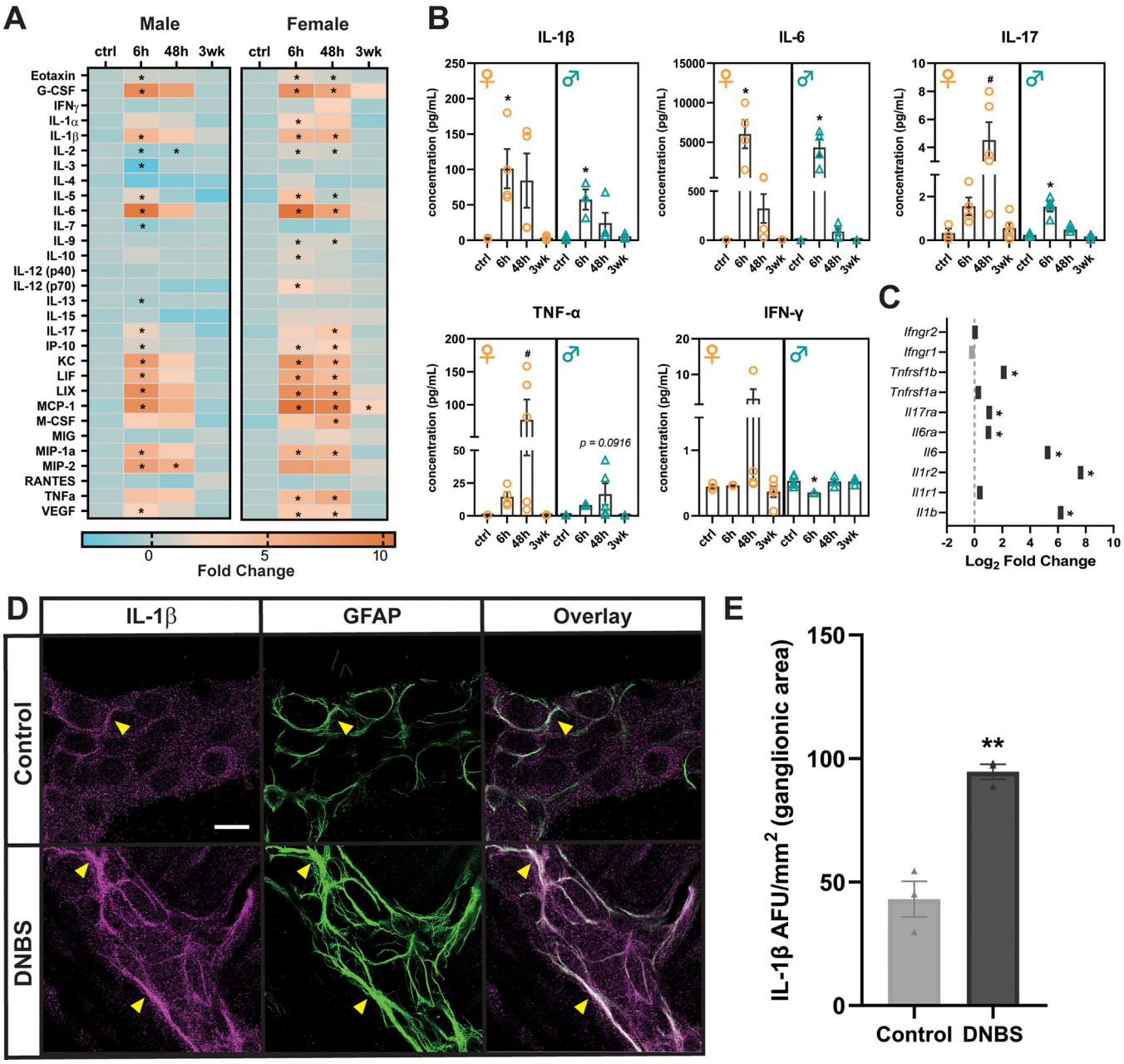

Figure 1. IL-1β expression is increased in enteric glia following inflammation.

(A) Heat maps showing the cytokine profile from whole colon tissue preparations over the time course of DNBS-induced colitis in male and female mice. Data are represented as fold change from control. **(B)** Concentrations in pg/mL of select cytokines in panel (A) from male (blue) and female (orange) mice at baseline (ctrl) or 6 hours, 48 hours, and 3 weeks after DNBS-induced colitis. One-way ANOVA followed by a Dunnett's multiple comparisons test, *p<0.05. Controls and treatment groups in (A and B) are each n = 3 to 5 mice per sex. **(C)** Bulk RNA-sequencing data sourced from Delvalle *et al.* (2) presented as Log_2 fold change in cytokine and receptor expression following DNBS-induced colitis at 48 hours. *p-adjusted < 0.1. Sequencing data were from n=3 mice. **(D and E)**

Representative confocal images showing overlay of double-label immunohistochemistry of glial marker GFAP and IL-1β within the myenteric plexus of colon from mice treated with saline (control) or DNBS, and quantification of IL-1β fluorescence intensity represented as arbitrary fluorescence units per ganglionic area (AFU/mm^2) from n = 3 mice in each group; *$p < 0.05$ by student's t-test (E). Yellow arrowheads denote colocalized GFAP and IL-1β labeling. Scale bar, 20 μm.

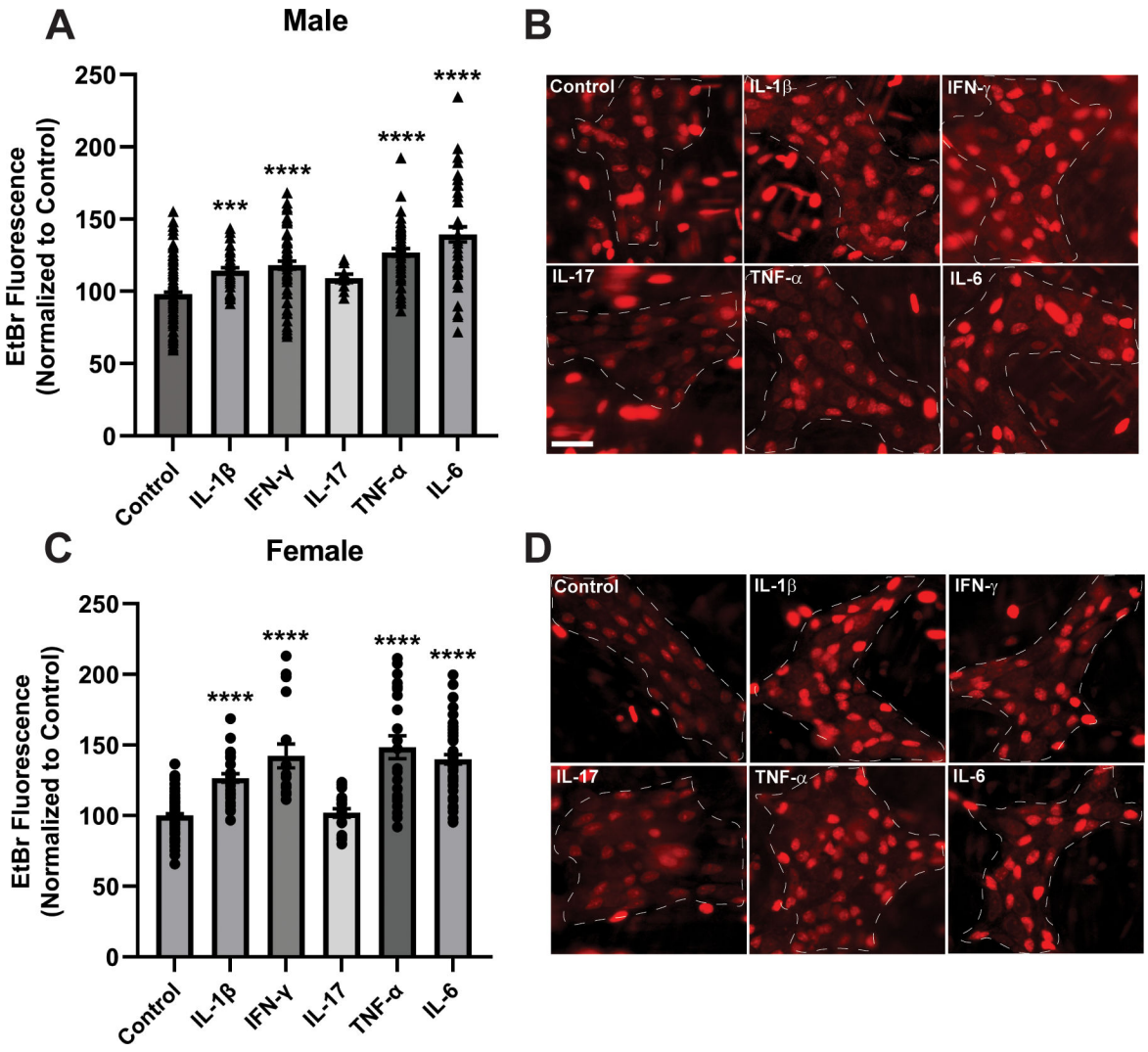

Figure 2. Impact of pro-inflammatory cytokines on glial dye uptake.

(A to D) Quantification and representative images of Cx43-mediated EtBr dye uptake in enteric glia within the myenteric plexus of male (A and B) and female (C and D) mice after stimulation with either IL-6, IL-17, TNF-α or IFN-γ relative to unstimulated controls. ***$p < 0.001$ and ****$p < 0.0001$ by one-way ANOVA followed by post-hoc analysis with a Dunnett's multiple comparisons test. Images are representative, and data are mean ± SEM from n = 10–15 ganglia from 2 to 3 mice each per group. Scale bar, 20 μm.

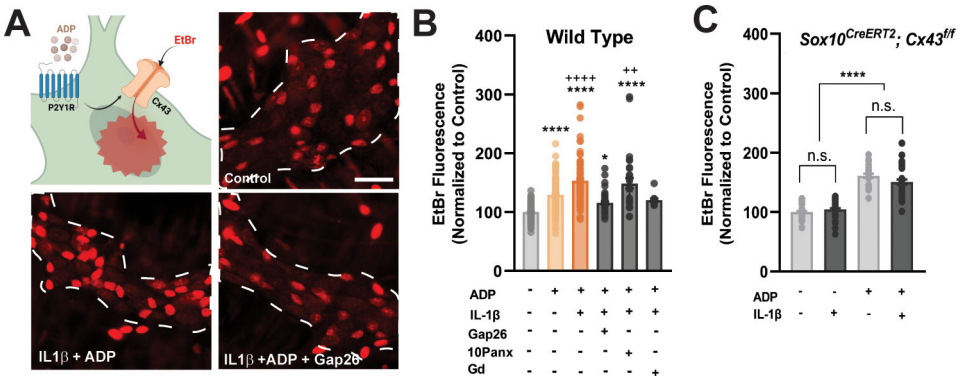

Figure 3. Effects of IL-1β on dye uptake through Cx43 hemichannels in ADP-stimulated enteric glia.

(A and B) Schematic diagram of the experimental paradigm and representative images (A) with quantification (B) of Cx43-mediated EtBr dye uptake in enteric glia within the myenteric plexus from wild-type mice in response to buffer (B, control; E, all "−") or ADP, ADP + IL-1β, or ADP + IL-1β and 43Gap26, 10Panx, or gadolinium (Gd). Results in the treatment groups were normalized to those of the control group. Scale bar, 20 μm. **(C)** Quantification of dye uptake as described and analyzed in (B), in *Sox10*^{cre}*ER*^{T2}*::Cx43*$^{f/f}$ mice in response to ADP with or without IL-1β. Quantifications in (B and C) represent pooled data from male and female mice, n = 10–25 ganglia from 3–4 mice each per treatment group. "n.s." not significant, *p<0.05 and ****p<0.0001 to control, and $^{++}$p<0.01 and $^{++++}$p<0.0001 to ADP, by ordinary one-way ANOVA followed by a Tukey's post-hoc test.

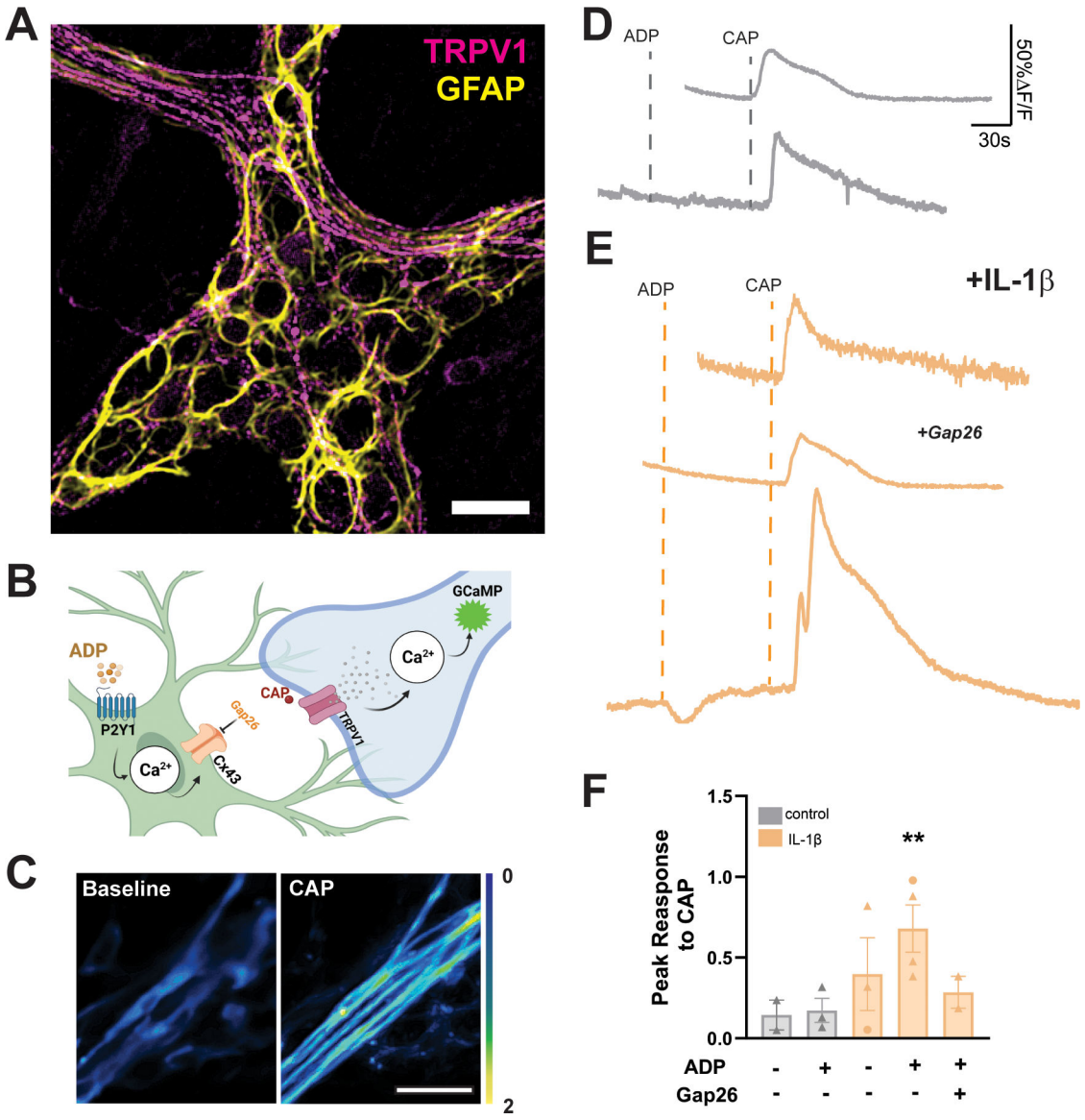

Figure 4. Enteric glia sensitize TRPV1+ nociceptors through Cx43-dependent mechanisms involving IL-1β signaling.

(A) Representative confocal image from *TRPV1Cre;GCaMP5g-tdT* mice colon whole mount preparations in which enteric glia were labeled with GFAP (yellow) and TRPV1+ nociceptors (magenta) labeled with tdTomato. **(B)** Schematic of the experimental paradigm. **(C)** Representative imaging of baseline and capsaicin (CAP)-provoked Ca^{2+} responses in nerve fibers from *TRPV1Cre;GCaMP5g-tdT* mice in isolated distal colon preparations. Scale bars, 20 μm. **(D to F)** Representative traces of average nerve fiber responses per ganglia, reported as ΔF/F over time (D and E), and quantification (F) of peak fluorescence values of control (gray) and IL-1β–treated tissue preparations (orange) in which enteric glia were stimulated with ADP and nociceptors were stimulated with capsaicin (CAP). Data (F) are mean ± SEM from n = average nerve responses from 5–7 ganglia from 3 or 4 mice per treatment group. Individual values were represented as triangles for males and circles

for females. **p<0.01 (to control) by ordinary one-way ANOVA followed by a Dunnett's post-hoc test.

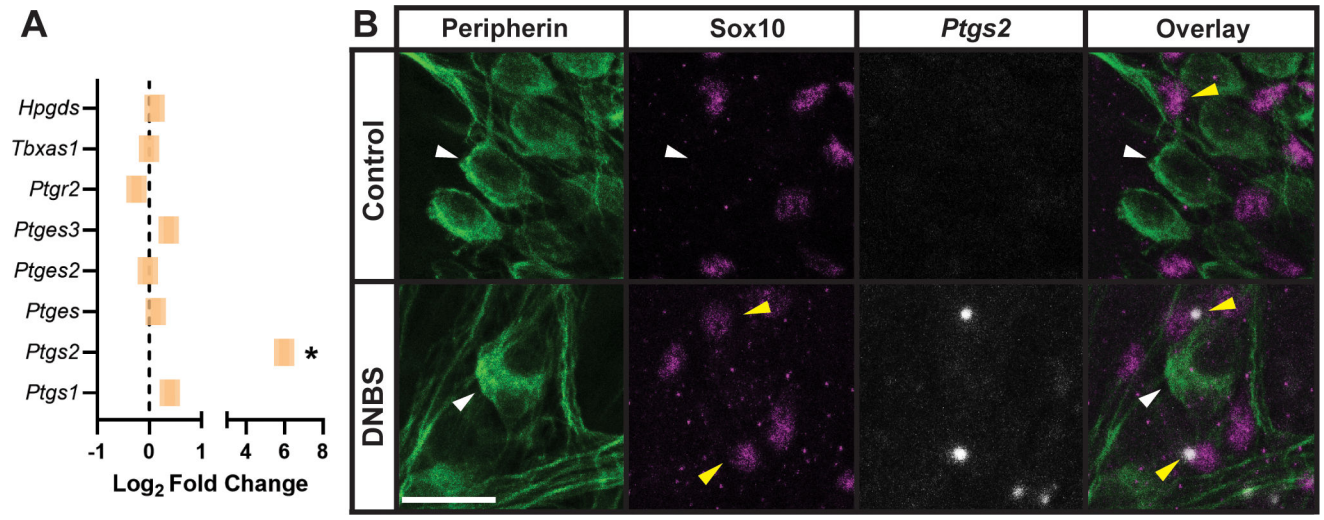

Figure 5. COX-2 expression is upregulated in enteric glia during colitis.

(A) Analysis of RNAseq data from Ribo-tag mice treated for 48 hours with either saline or DNBS (2) represented as Log_2 fold change [differential expression analysis (DESeq2)]. *p<0.1, n=3 male and female mice. **(B)** Representative confocal images of myenteric ganglia from either control mice (top panels, n=4 male and female mice) or mice treated for 48 hours with DNBS (bottom panels, n=4 male and female mice), labeling *Ptgs2* RNA (gray) with RNAscope followed by IHC labeling neurons with peripherin (green) and glia with Sox10 (magenta). Neurons are highlighted by white arrows and enteric glia are indicated by yellow arrows. Scale bar, 20 μm.

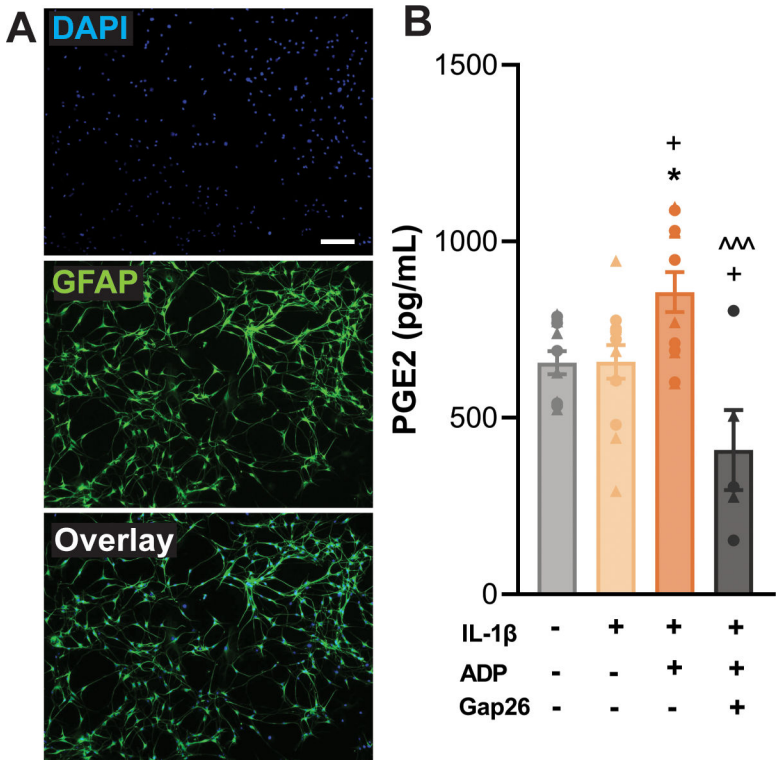

Figure 6. Stimulated enteric glia release PGE_2 in the presence of IL1β.

(A) Representative images of primary enteric glia cultures labeled with GFAP. Scale bar, 50 μm. **(B)** Quantification of PGE_2 release from enteric glia in cell culture supernatants treated with IL-1β and stimulated with ADP in the presence of 43Gap26. Data are from n = 5 to 12 mice, in which individual values are represented as triangles for males and circles for females, and analyzed by ordinary one-way ANOVA followed by a Tukey's post-hoc test: *$p<0.05$ to control, $^{+}p<0.05$ to IL-1β only, and ^^^$p<0.001$.

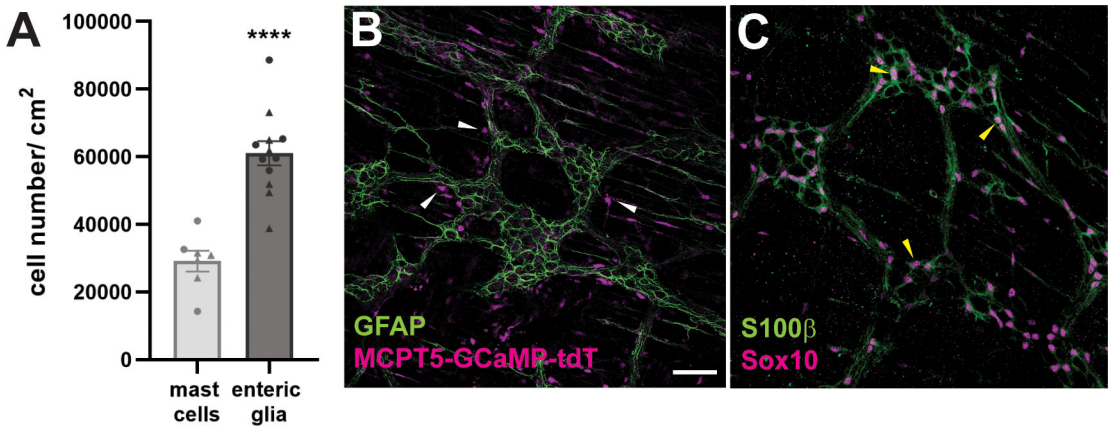

Figure 7. Relative abundance of enteric glia and mast cells at the level of the myenteric plexus.

(A to C) Quantification (A) and representative confocal images of glial (C) and mast cell (B) numbers within the myenteric plexus. tdTomato-positive mast cells are indicated by white arrows and Sox10+ enteric glia are indicated with the yellow arrow. Mast cells were quantified in *MCPT5-GCaMP-tdT* mice and were identified by tdTomato labeling. GFAP immunolabeling was used to identify myenteric ganglia. Enteric glia were identified and quantified via immunohistochemistry with S100β and Sox10 in wild-type mice. Individual values represented as triangles for males and circles for females. Data are from n = 7 to 12 mice and were evaluated with a Student's t-test: ****$p < 0.0001$. Scale bar, 50 μm.

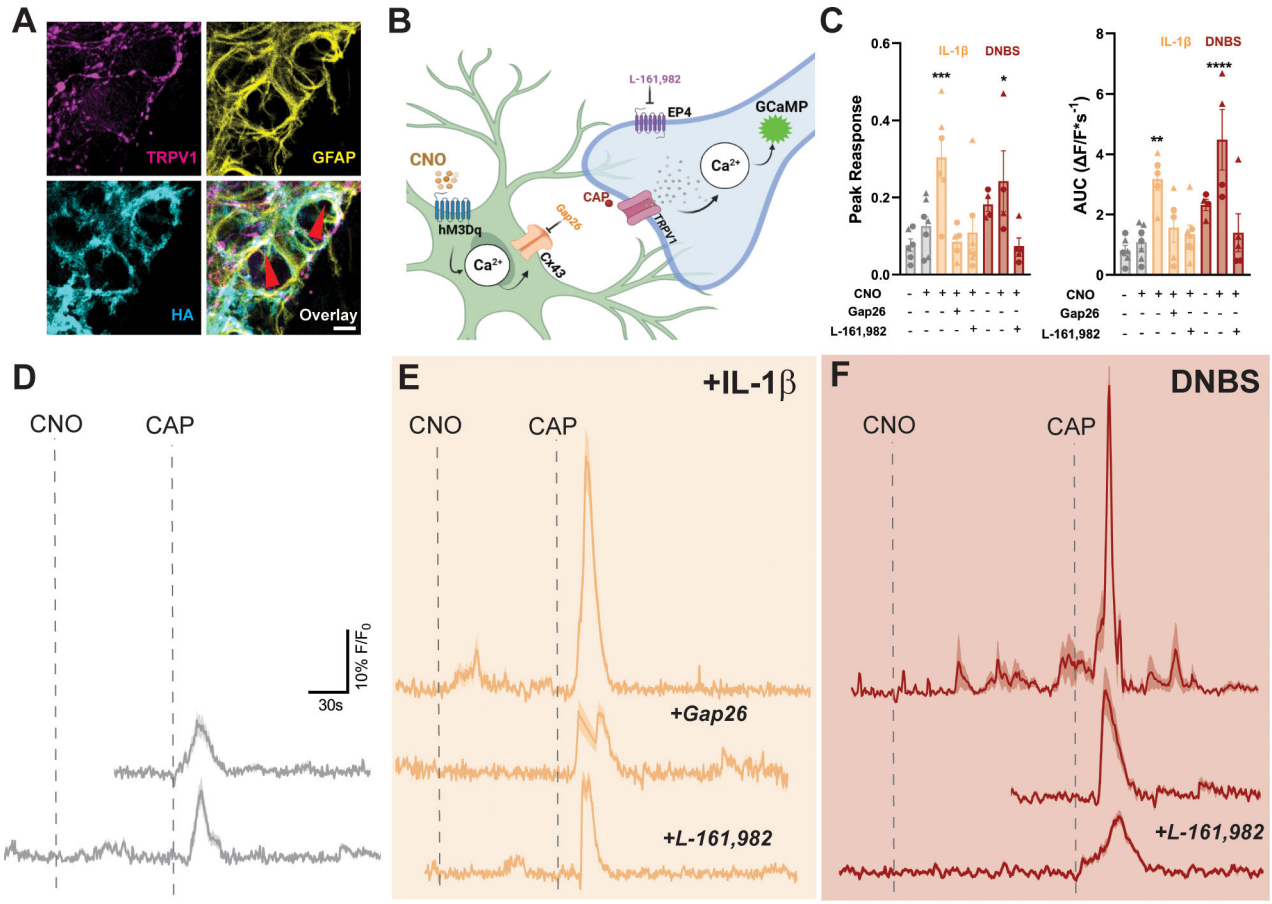

Figure 8. Enteric glia sensitize nociceptors through the Cx43-dependent release of PGE_2.

(A) Representative confocal images assessing co-localization of the HA-tagged hM3Dq receptor (cyan) on GFAP-labeled enteric glia (yellow) and tdTomato-labeledTRPV1+ nerve fibers (magenta) from *GFAP-HM3Dq;TRPV1Cre;GCaMP5g-tdT* mice whole mount preparations. Red arrows highlight areas of colocalization between GFAP and HA. Images are representative of n = 4 male and female mice. Scale bar, 20 μm. **(B)** Schematic of the experimental design. **(C to F)** Quantification (C) and representative traces (D to F) of peak fluorescence values and AUC averaged from nerve fibers per ganglia of control (gray), IL-1β (orange), and DNBS (1wk, red) treated isolated colon preparations. Enteric glia were stimulated with CNO and nociceptors were stimulated with capsaicin (CAP). Representative traces are reported as ΔF/F over time. Data are mean ± SEM from n = 4–7 ganglia from 3 to 4 mice per treatment group, in which individual values are represented as triangles for males and circles for females. Data were analyzed by ordinary one-way ANOVA followed by Dunnett's post-hoc test: *p<0.05, **p<0.001, ***p<0.001, and ****p<0.0001 to control.

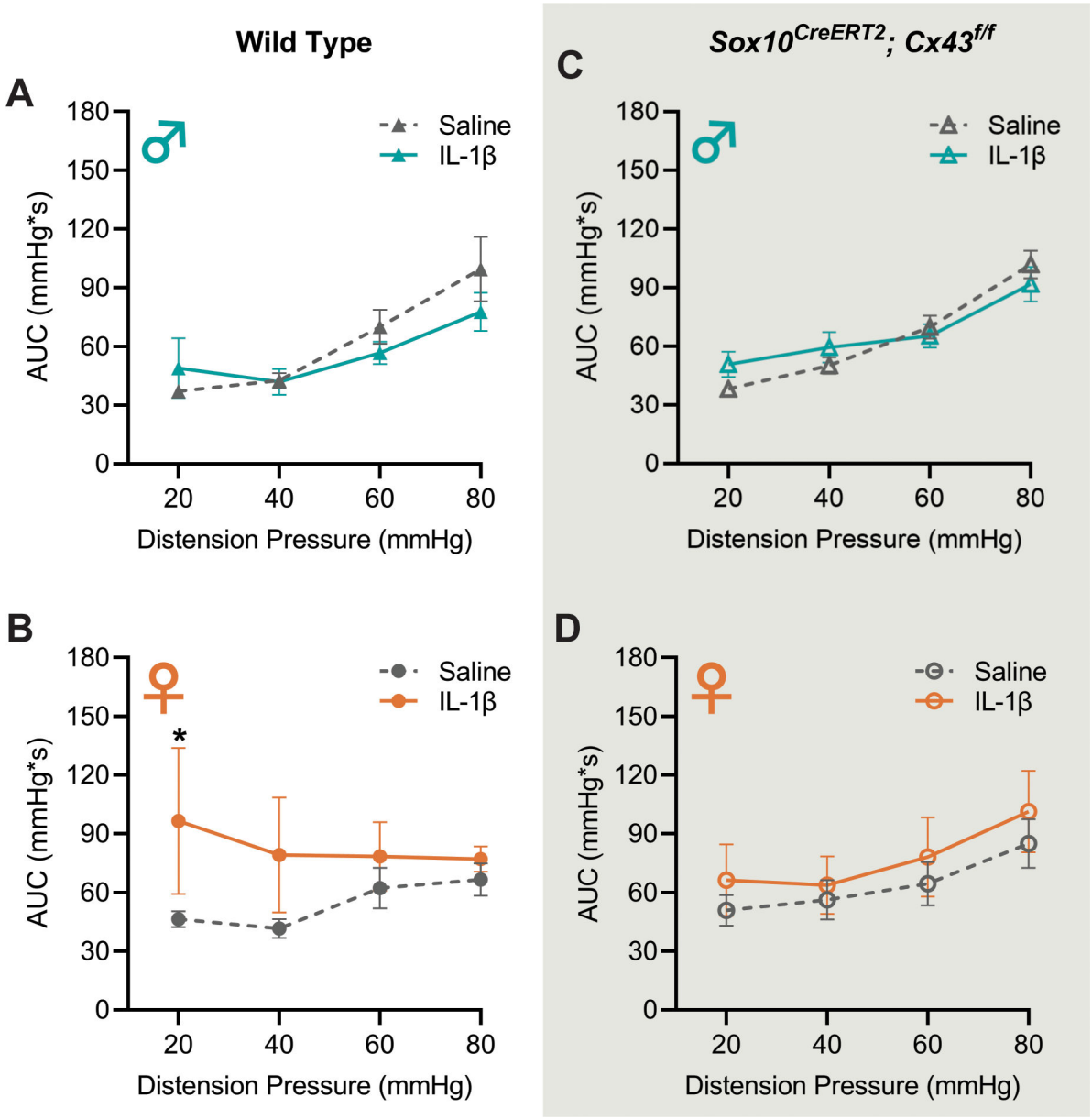

Figure 9. Enteric glia impact afferent nerves and integrated reflexes through a Cx43-dependent mechanism.

(A to D) Traces showing VMR responses to colorectal distension in mice shown as the area under the curve (AUC) for each distension pressure. Data show VMR responses in both male (blue) and female (orange) mice in wild-type (A and B) or *Sox10*^{cre}*ER*^{T2}*::Cx43*$^{f/f}$ (C and D) mice following treatment of a saline or IL-1β enema. AUC values for each group, from n = 6 to 9 mice, were analyzed via repeated measures two-way ANOVA followed by a Bonferroni's post hoc analysis: *p < 0.05.